Long-term stability, noise, and temperature sensitivity of modular porous-pot electrodes designed for geophysical and geotechnical applications, and details of their construction

Comeau, Matthew J.; Ueding, Stefan; Becken, Michael

DOI
10.1029/2023EA003327

Publication date
2024

Document Version
Final published version

Published in
Earth and Space Science

Citation (APA)
Comeau, M. J., Ueding, S., & Becken, M. (2024). Long-term stability, noise, and temperature sensitivity of modular porous-pot electrodes designed for geophysical and geotechnical applications, and details of their construction. *Earth and Space Science*, *11*(2), Article e2023EA003327. https://doi.org/10.1029/2023EA003327

Earth and Space Science

RESEARCH ARTICLE
10.1029/2023EA003327

Long-Term Stability, Noise, and Temperature Sensitivity of Modular Porous-Pot Electrodes Designed for Geophysical and Geotechnical Applications, and Details of Their Construction

Matthew J. Comeau[1], **Stefan Ueding**[2], **and Michael Becken**[2]

[1]Delft University of Technology, Department of Geoscience and Engineering, Delft, The Netherlands, [2]Universität Münster, Institut für Geophysik, Münster, Germany

Key Points:

- Development of a modular, repairable, refillable porous-pot electrode with an over-saturated electrolyte, preferably stabilized in clay
- Long-term measurements reveal (a) high stability, (b) smooth drift, <0.5 mV/month, and (c) low noise, 0.2–0.4 μV at a period of 1–120 s
- Experiments from −3 to 35°C determine a temperature sensitivity of the electric potential of about −30 μV/°C, which is considered low

Correspondence to:

M. Becken,
michael.becken@uni-muenster.de

Citation:

Comeau, M. J., Ueding, S., & Becken, M. (2024). Long-term stability, noise, and temperature sensitivity of modular porous-pot electrodes designed for geophysical and geotechnical applications, and details of their construction. *Earth and Space Science*, *11*, e2023EA003327. https://doi.org/10.1029/2023EA003327

Received 4 OCT 2023
Accepted 16 JAN 2024

Author Contributions:

Investigation: Matthew J. Comeau
Methodology: Stefan Ueding
Resources: Michael Becken
Writing – original draft: Matthew J. Comeau

Abstract Electrodes are used to measure a potential difference between two points. In geophysical and geotechnical applications they are often in the form of non-polarizable porous-pot electrodes. Here we describe the design, construction, and testing of modular and refillable electrodes, which facilitates repair as the electrodes degrade over time. We use a chemical composition based on a metal in contact with an over-saturated electrolyte that consists of a salt of that metal and an auxiliary salt. We compare characteristics when the electrolyte is stabilized in a clay or not, and with various states of ceramic porous plugs and two types of wood plugs. Next, we assess the long-term stability (more than 1 month), noise (periods of 1 s to 1 hr), and temperature sensitivity of different types of electrodes. Electrodes with an electrolyte and clay formula showed lower noise (0.2–0.4 μV at periods of 1–120 s), greater long-term stability (0.05–0.5 mV/month of smooth drift), and greater consistency between samples measured than those with no clay (noise and drift values up to four times larger). The effects from different porous plugs were negligible, with similar results for ceramic and wood types. The temperature sensitivity of the electric potential was assessed, from −3 to 35°C. All electrodes showed a temperature sensitivity of about −30 μV/°C. This is considered very low compared to some commercially available electrodes. Finally, continuous long-term laboratory and field measurements of the potential highlight the application of the new electrodes.

1. Introduction

Non-polarizable porous-pot electrodes are used to measure a potential difference (voltage) between two points on the Earth, from which telluric currents are generated (Figure 1). They can be used for geophysical and geotechnical applications such as magnetotellurics, controlled-source electromagnetic induction experiments, and self-potential measurements, as well as for induced polarization and electrical resistivity tomography experiments. Measurements may be carried out for long periods on the order of several days, for example, for magnetotelluric measurements, or for short periods on the order of minutes, for example, for controlled-source electromagnetic induction experiments, as well as for static measurements. A non-polarizable electrode has a potential that is not affected by the passing current. Undoubtedly it is electrode noise and stability that will limit the quality of any measurement of the electrical field within the Earth. Within an electrode, the contact between the electrolyte fluid and the metal wire (internal; which transmits the potential of an ionic conductor to an electronic conductor) can create potentials in addition to those created in the surroundings or soil (external), and if they are not small or are not stable they can disturb or contaminate the measurement of the potential difference between a pair of electrodes along a telluric dipole (Petiau & Dupis, 1980).

Various electrode types are possible, including copper–copper(II) sulfate (Cu–$CuSO_4$), silver–silver chloride (Ag–AgCl), and lead–lead(II) chloride (Pb–$PbCl_2$), in which a metal and metal-salt are combined. Petiau (2000) showed that lead–lead(II) chloride electrodes with a saturated electrolyte stabilized in a clay with a controlled internal pH were particularly stable. In this study, we describe the design and construction of a modular, refillable, porous-pot electrode with a chemical composition based on that described by Petiau (2000). In this study we (a) compare the characteristics of different electrode types (with and without a clay base and different types of porous plugs, ceramic or wood), (b) measure the sensitivity of the potential recordings to temperature, (c) assess the

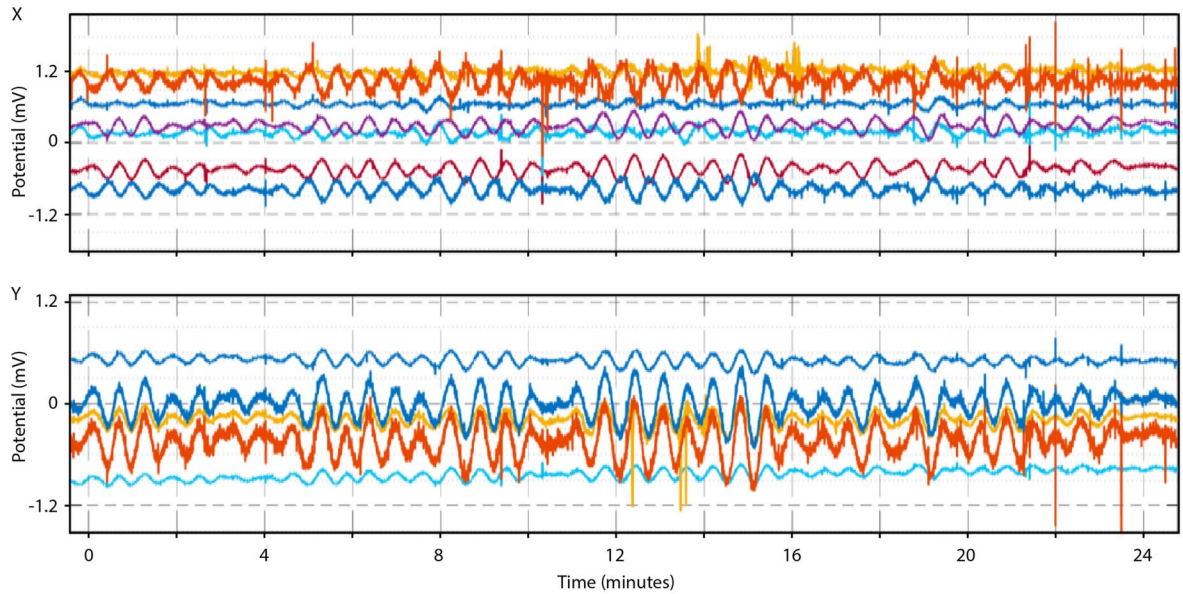

Figure 1. Time series of the electric potential for a geophysical study. Shown are simultaneous recordings at many separate locations (colors). Measurements were made with the porous-pot electrodes discussed here (type 1). The fields were recorded in two orthogonal horizontal directions (X, north–south; Y, east–west), with 60m dipole lengths. For the magnetotelluric technique, electric field data are combined with simultaneous magnetic field recordings. Data come from measurement locations in the Khovsgol region of northern Mongolia, approximately 50°N and 100°E (Rigaud, Comeau, Becken, et al., 2023, Rigaud, Comeau, Kuvshinov, et al., 2023): n6120, n6100, n6160, n8060, n8070, n8080, n8100, n8105, and s030. Geomagnetic pulsations are observed (Pc3, about 40s period). The sampling rate shown here is 8Hz. Time is measured in minutes from 9:40:0 16 August 2022.

short-period (1–120 s) noise of different electrode types, and (d) assess the long-term (days, months) stability of the electrodes.

2. Construction and Design of a Modular Non-Polarizable Porous-Pot Electrode

2.1. Design of the Pot

The design principle was one of modular components which can be disassembled and individually repaired, replaced, and refilled at regular intervals. This helps to reduce waste overall. In particular, the electrolyte solution within the electrode degrades over time. The pots were designed by the University of Münster from 2014 to 2016. The body of the electrode is constructed from simple plastic tubing (see Figures 2 and 3). We use a diameter of 75 mm, but this can be varied. We prefer a wall thickness of 5.6 mm, as this adds insulation and robustness to the design. The inner chamber has a height of about 130 mm and the total height is about 165 mm, but it could be adjusted as required. The top consists of a threaded plastic disc that ensures the pot can be easily opened for maintenance and repair. In contrast, most commercially available porous-pot electrodes use a glue, which makes refilling the electrodes impossible or difficult. There is a pressure release screw on the top disc, to equilibrate internal and external pressure after closing the assembly. The basic pot design described here is similar to the design used by the Geophysical Device Pool Potsdam (GIPP) and the Geomagnetic Observatory in Niemegk for silver–silver chloride electrodes. The design described here can work for several electrode types, including lead–lead(II) chloride (Pb–$PbCl_2$), copper–copper(II) sulfate (Cu–$CuSO_4$), and silver–silver chloride (Ag–AgCl).

The top disc has a threaded hole to securely attached a metal rod (e.g., a lead tube, a silver pellet, copper coil, etc.), which is connected to a copper cable inserted through the top disk by means of a plug connector (see Figure 2). For a good connection we use a gold-plated connector at the end of the copper cable. This is set in a plastic housing and sealed with a rubber O-ring and a flexible neck so that the copper cable does not easily bend or break. Having the copper cable plug directly and securely into the rod is a unique feature of the design and is more reliable than the typical method of soldering. We use a machined metal rod, with a wall thickness of 3 mm, a

10.1029/2023EA003327

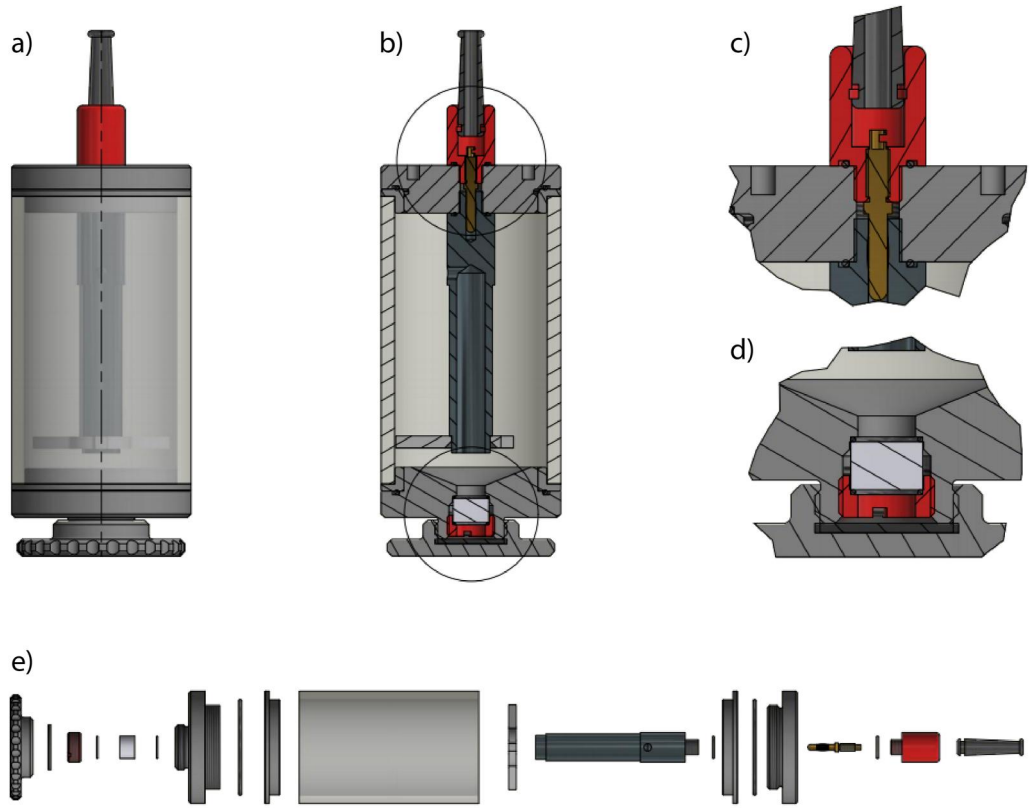

Figure 2. Technical rendering of the modular non-polarizable porous-pot electrode design. Panels show: (a) the full electrode, with transparency, (b) a cut-away view showing the interior of the electrode (circles indicate c and d), (c) the top part with the copper cable and gold-plated connector inserted into the metal rod (scaled 200% compared to a), (d) the bottom part with the porous plug and storage cap (scaled 200% compared to a), and (e) an exploded view from the side showing all the pieces (left to right: plastic threaded cap, rubber insert mat, threaded plastic holder for porous plug, rubber O-ring, porous plug, O-ring, threaded bottom disc with O-ring, plastic pipe for the pot or electrode body, plastic stabilizer for the metal tube or rod, lead tube, O-ring, threaded top disc with O-ring, gold-plated connector plug, O-ring, connector for copper cable, flexible neck) (scaled 60% compared to a).

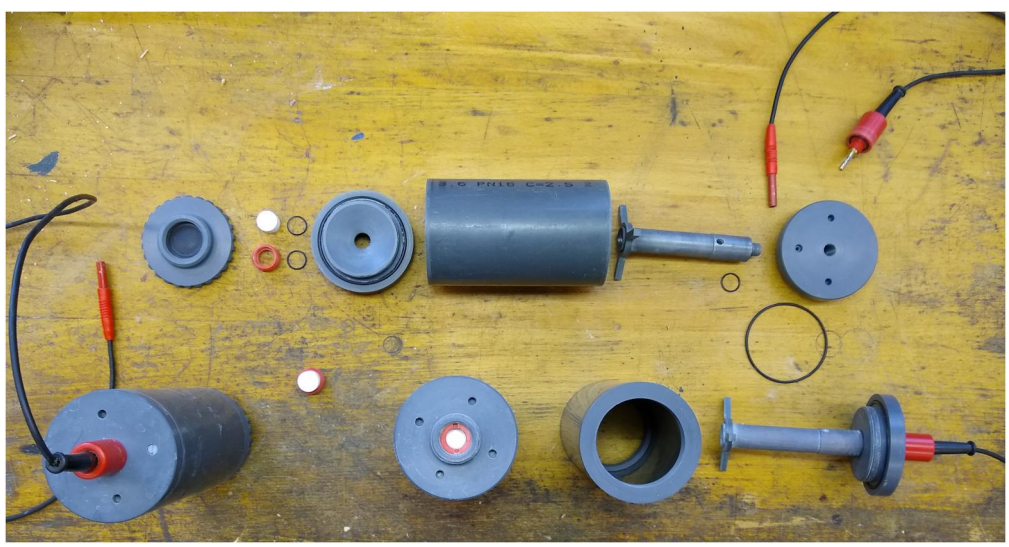

Figure 3. Photograph of the various parts of the modular porous-pot electrode design. Confer with the technical drawing in Figure 2.

Figure 4. Photograph of the lead tubes before and after cleaning. Due to the modular design, the lead tube can be removed, cleaned, and re-installed with ease. Two used or dirty tubes are on the left and two clean tubes are on the right. The plastic stabilizer at the bottom keeps the tube in position in the pot and helps preserve the shape.

diameter of 18 mm, and a height of 100 mm. Because of the modular design, the copper cable can be replaced easily and quickly (simply by unscrewing it) if it becomes damaged, as can occur readily in the field (e.g., by grazing animals). Similarly, the metal rod can be regularly removed, cleaned, and re-installed with ease (Figure 4).

The bottom consists of a plastic disc that contains a threaded chamber, constricted to 11 mm diameter at the narrowest inside, where a (weakly) porous plug is fitted, sealed with rubber O-rings both above and below (see Figure 2). We use a porous plug with a diameter of 10.3 mm and a height of 15.2 mm. Petiau (2000) reported a strong increase in the dis-saturation time of the electrode (on the order of a factor of 100) when using a narrow channel in the electrode pot design. If possible, the porous plug is preferably flush with the outside of the electrode pot, to ensure good ground contact; if it is set inside too deep then care must be taken at installation that it remains in contact with the soil (no air gaps), or soil/mud must be placed inside it. A removable threaded plastic cap covers this when in storage and is filled with a small volume of salt water (KCl; about 10 mL) to keep the electrode in a sealed and moist environment to prevent drying out of the electrolyte.

2.2. Characteristics of the Porous Plug

The porous plug we prefer is a ceramic, manufactured as a pressed clay pellet, because it is chemically inert and has a low thermal conductivity. It has a density of about 2,700 kg/m^3 (5.0 g per pellet). It has a water flow-through rate in air of less than 0.1 mL/day, measured at 20°C. This was measured over 5 days (from 17 November 2022) with the open pot filled with water and suspended in air. The water flow-through rate in sand, measured in a bucket with 4 kg of dry sand, is approximately 10 mL/day, measured at 20°C over 3 days (Table 1). A dirty pellet that had been used for several years was found to have a flow-through rate of 80% of that of a new ceramic pellet. Because of the modular design, the porous plug can be removed, cleaned, and re-installed without deconstructing the electrode pot or removing the electrolyte. Over time, salts permeate the surface layer of the ceramic leading to discoloration and pore blockage (Figure 5). When the pellet was cleaned, first in an ultrasonic bath with warm water (Figure 6) and then with a diamond-tipped lathe to shave off 0.1 mm of the surface, it was found to have a flow-

Table 1
Water Flow-Through Rate in Sand for Porous Plugs

Type	Rate (mL/day)	Ratio to new
New ceramic	10.4	1.00
Cleaned ceramic	9.7	0.93
Dirty ceramic	8.3	0.80
Spruce wood	7.7	0.73
Oak wood	7.0	0.67

10.1029/2023EA003327

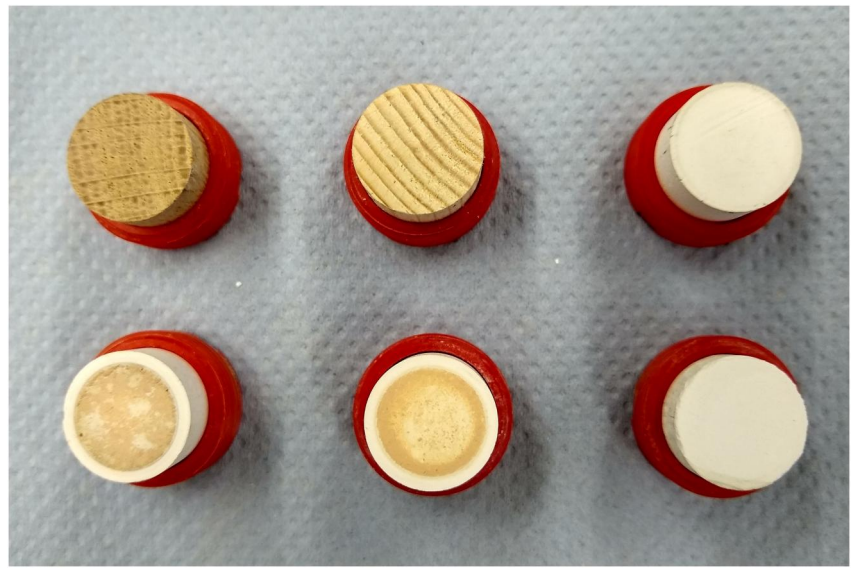

Figure 5. Photograph of the porous plugs used. From top left to bottom right they are, (a) oak wood, (b) spruce wood, (c) new ceramic, (d) dirty used ceramic, (e) dirty used ceramic, (f) cleaned ceramic.

through rate of about 93% of that of a new ceramic pellet. A weakly porous plug can help to increase the dis-saturation time of the electrolyte in the electrode (Petiau, 2000).

Alternatively, we tested wood plugs (see Figure 5). These were manufactured from spruce wood and oak wood. They have a density of about 430 kg/m^3 (0.8 g per pellet) for spruce and 650 kg/m^3 (1.2 g per pellet) for oak. They have a water flow-through rate in air of about 50% (spruce) to 10% (oak) of that of the ceramic pellet described above. Their water flow-through rate in sand was about 73% (spruce) to 67% (oak) of a new ceramic pellet (see Table 1), or about 92% (spruce) to 83% (oak) compared to a dirty or used ceramic pellet. Our measurements show that wood porous plugs are a suitable alternative to ceramics.

Figure 6. Photograph of the process of cleaning the ceramic pellets in a warm ultrasonic bath. The photographs show the time progression from left to right (0 s, 4 s, 200 s; note that the water has become clouded with contaminants).

Table 2
Chemical Composition of Electrodes

Component	Amount
H_2O, Water	1 L
$PbCl_2$, Lead(II) chloride	40 g
KCl, Potassium chloride	680 g
HCl, Hydrochloric acid (33%)	3.7 mL
Clay powder, Kaolin/Bolus (2.6 g/cm^3)	1.65 kg

Note. This recipe is based on Petiau (2000). It is enough to fabricate about eight electrodes of the design discussed.

2.3. Chemical Composition of a Saturated Electrolyte Stabilized in a Clay

The electrode contains a metal and a salt of that metal. We follow the composition determined by Petiau (2000) and focus on a lead–lead(II) chloride electrode, although it is possible to keep the same basic design and use a different composition (for the salt and metal). An electrolyte is created by combining a principal salt (lead(II) chloride, $PbCl_2$, which is very weakly soluble) with an auxiliary salt (here we use potassium chloride, KCl, which contains the same anion) in solution. Note that Petiau (2000) refer to these as second generation electrodes or electrodes of the second kind, and those with no auxiliary salt as first generation electrodes. The electrolyte is strongly over saturated (by a factor of about four for the primary salt and two for the auxiliary salt; solubility of $PbCl_2$ is about 10 g/L and of KCl is about 340 g/L, at 20°C). A dry powdered clay (e.g., Kaolin/Bolus, density of 2.6 g/cm^3; CAS registry number 1332-58-7) is directly mixed with the liquid electrolyte to stabilize it. This forms a thick mud that is homogenous and that contains non-dissolved salts distributed throughout, due to the over-saturated electrolyte. The internal pH of the electrolyte is controlled by the addition of an acid (hydrochloric acid, HCl), and adjusted to a pH of 4–5, where it has been found to be most stable (Petiau, 2000). Petiau (2000) reported that the time of dis-saturation was increased by nearly of factor of two when using clay. Over time, capillary suction will result in the removal of electrolytes from the clay inside the electrodes, and, consequently, the measured electrode potential may increase (Petiau, 2000). When buried in soil, the diffusion of ions between the ground and the electrodes (an attempt to equilibrate the ion concentrations) results in a decrease in the ion concentration within the electrode, but the non-dissolved salt in the clay can keep the saturation and therefore keep the electrode potential constant (Petiau, 2000). Analysis by Petiau (2000) shows that this time span may be months to tens of years. In our experience, refilling the electrolyte solution is advisable every few years when used yearly for lengthy measurement campaigns, but, when stored properly, in principle will last much longer. Our experience from one batch was a 7.5% failure rate after more than 2 years with repeated field installations and in total several months of recording time.

The specific chemical composition is given in Table 2. We used laboratory-grade materials (98%–99.9% purity); however, Petiau (2000) notes that lead electrodes are very weakly sensitive to impurities, in contrast to, for example, silver electrodes. The KCl can be replaced with NaCl (sodium chloride; ratio of 34:36, based on solubility; solubility of NaCl is about 340 g/L at 20°C); however, Petiau (2000) determined that acceptable noise and stability in this case is over a narrow range of pH and the temperature coefficient is much higher. The electrolyte and clay formula is prepared, mixed vigorously, and then let sit for one or more days in order to equilibrate before the pots are filled. The consistency is that of a wet mud or gelato (Figure 7). For the design discussed, about 400 g of the electrolyte and clay formula are inserted into each pot; in that case, the recipe in Table 2 makes eight electrodes.

Figure 7. Photograph of the saturated electrolyte stabilized in a clay. The consistency is that of a wet mud or gelato.

3. Measurements of Resistance and Potential

3.1. Comparison Between Electrode Types

New electrodes were constructed (November 2022), including: (a) many (20 in the first batch and 16 in the second batch) with the above saturated electrolyte and clay formula and ceramic porous plugs (which we call type 1), (b) two new electrodes with the electrolyte and clay formula and wood porous plugs (type 1b), (c) three new electrodes with the electrolyte only (no clay) and ceramic porous plugs (type 2), and (d) two new electrodes with the electrolyte only (no clay) and wood porous plugs (type 2b). They were compared to four old type 1 electrodes that had been used for some years (constructed 2+ years prior).

Table 3
Resistance and Potential of Electrodes

Type	Samples	Resistance (Ω)		Potential (mV)
		Range	Mean	Range
Old, electrolyte and clay, used ceramic plug (type 1)	4	340–450	410	0.5–1.5
New, electrolyte and clay, ceramic plug (type 1)	20	335–580	430	0.1–3.0
New, electrolyte and clay, ceramic plug (type 1)	16	305–550	428	0.1–1.2
New, electrolyte and clay, wood plug (type 1b)	2	444–453	449	0.2–0.6
New, electrolyte only, ceramic plug (type 2)	2	190–190	190	1.7–2.9
New, electrolyte only, dirty ceramic plug (type 2)	1	200	200	1.7
New, electrolyte only, wood plug (type 2b)	2	180–250	215	2.8–3.0

Note. Measurements in salt water (KCl with 5% saturation; temperature of 22°C).

The resistance and potential of all was measured in a bucket of salt water (KCl with 5% saturation) at room temperature (about 22°C) against a reference electrode. The resistance was measured with an impedance meter (Sennheiser) set to 1,000 Hz. The new electrolyte and clay electrodes with ceramic plugs (type 1) had resistances in the range of 305–580 Ω, with a mean of about 430 Ω. Their potentials were in the range 0.1–3.0 mV. The old electrolyte and clay electrodes with ceramic plugs had similar values: 340–450 Ω with a mean of about 410 Ω and potentials in the range 0.5–1.5 mV. This indicates that the electrodes are good for some years, without maintenance. See Table 3 for a summary.

The electrolyte and clay electrodes with wood plugs (type 1b) measured 453 Ω (spruce) and 444 Ω (oak), with potentials of 0.2 and 0.6 mV. Therefore, there was no significant difference found in the resistance and potential compared to electrodes with ceramic plugs.

The electrodes with electrolyte only (no clay) had a resistance lower than the others, with all those with ceramic plugs (type 2) having 190–200 Ω and those with wood plugs (type 2b) measuring 180 Ω (spruce) and 250 Ω (oak). This is 40%–55% of the value when using the electrolyte and clay formula. The electrodes with electrolyte only (no clay) were found, in general, to have a higher potential than the electrodes with the electrolyte and clay formula, 1.7–2.9 mV for ceramic plugs and 2.8–3.0 mV for wood plugs (Table 3).

In another test we compared a dirty or used ceramic plug and a clean one in a new electrode with electrolyte only (no clay) by directly replacing only the plug and keeping the other parts of the electrode the same (a benefit of the modular design). The resistance and potential were found to be not significantly different: when the dirty ceramic plug was directly replaced with a cleaned ceramic plug the resistance was found to decrease very slightly, by just over 5%.

Stating the conditions under which such measurements are made is imperative because they are sensitive to variables including the temperature (see Section 3.2 below where this is explored in detail) and the medium where the measurement is taking place (whether in water or soil) and the concentration of salts or ions in the medium. To highlight this, we varied the quantity and thus concentration of KCl salt in a bucket of water where a pair of electrodes were situated and compared their electrical resistance (Figure 8). The measurements were made over a time span of 28 days (from 6 February 2023), and included regular measurements with a voltmeter and an impedance meter. The experiment was repeated three times. It was observed that the electrodes need time to reach equilibrium with the solution and with each other, often several hours (typically a sharp decrease in the first hour is followed by about 6 hr of gradual rise, as the local salt concentrations are distributed and homogenized in the water over time). Thus measurements were made one or two full days after any change to account for stabilization, and were repeated several times. The potential was found to be very stable for the subsequent measurements. It had a mean of −0.18 mV with a standard deviation of 0.03 mV throughout the timeframe. For a concentration of 5% KCl (17 g/L), the resistance was 302 Ω; it decreased to ∼100 Ω for a concentration of 20% KCl (68 g/L). The value for 0% (only in tap water) was ∼1,960 Ω.

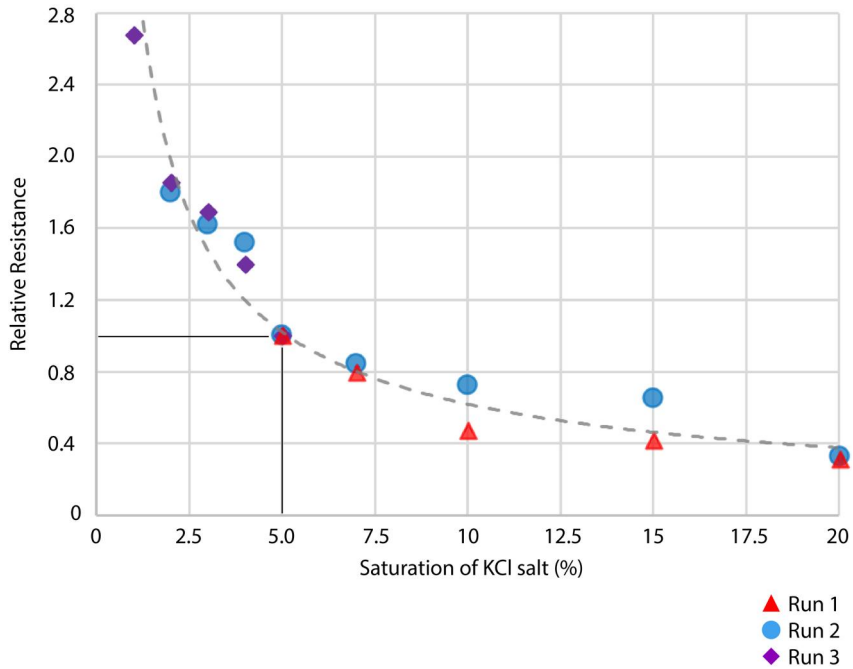

Figure 8. The electrical resistance for a pair of electrodes in salt water with the quantity of KCl salt varying. A concentration of 3.4 g/L is taken to be 1% saturation and 34 g/L to be 10% saturation. A relative resistance is shown, with the value of 1.0 taken to be the value at 5% saturation (17 g/L), which in this example was 302 Ω. The value for 0% (only in tap water) was ~1,960 Ω, giving a relative resistance of ~6.5 (not shown). The trendline shown is a power function ($y = 3.26x^{-0.72}$; best fit R-squared value of 0.93). Different colors denote different measurement runs, repeated with the same electrode pair but in different buckets at different times.

3.2. Variations With Temperature

The electrodes have a temperature dependence that is attributed to the temperature dependence of the complex chemical reactions that occur at the surface of the electrode. This effect is significant for measurements made over long time frames that may capture large swings in the temperature, for example, daily variations or seasonal variations that can be tens of degrees. Four electrodes were placed in a (Vötsch) temperature-controlled climate chamber (see Figure 9) and the resistance and potential of the electrodes in a bucket of salt water (KCl with 5% saturation, about 17 g KCl in 1 L of water) was measured through a plug in the apparatus against a reference electrode. The measurements were made over a time span of 15 days (from 17 November 2022) and included both continuous monitoring with a data logger (described by Becken et al., 2014; sampling rate of 128 Hz) and periodic measurements with a voltmeter and an impedance meter (Sennheiser; at 1,000 Hz). The temperature was varied systematically from 0 to 35°C. The temperature was both increased and decreased, to avoid effects such as drift. Measurements were made 1 or 2 days after a temperature change to account for stabilization, and were repeated several times (e.g., hourly, when possible). It was observed that for large temperature variations (e.g., changing from 20 to 10°C or from 5 to 20°C) the potential oscillated (one or more peaks/troughs with variations on the order of 0.1–0.7 mV) over a period of about 10 hr, followed by about 20 hr of smooth, gradual change before becoming stable and repeatable.

It is observed that the resistance increases as the temperature decreases (Figure 10). For the electrodes with the electrolyte and clay formula and ceramic plugs (type 1) and for a subset of the data, from 5 to 30°C, a linear slope can be approximated. A best fit line shows a close fit to the data with an R-squared value above 0.87. The liner slope is −25 (units of Ω/°C) for electrode #9 and −20 for electrode #21 (others tested followed a similar pattern). For the whole range of temperatures, particularly the lower temperatures, an exponential function fits the data better. An additional measurement was carried out for the extreme case of −3°C, where the water medium was partially frozen into ice, and showed that the resistance increased as high as 10,100 Ω. Throughout the experiment, repeated measurements at the same temperature showed similar values for each individual electrode: the

Figure 9. Photograph of the (Vötsch) temperature-controlled climate chamber where measurements of the temperature sensitivity of the electrodes were carried out.

standard deviation ranged from less than 1%–8% of the (mean) value, with a total average of about 3% (e.g., a standard deviation of 1–6 Ω for measurements at 30°C and 30–50 Ω for measurements at 5°C, with a measurement separation of 1 hr to 1 day).

It is observed that the potential increases as the temperature decreases (Figure 11). We analyzed data from the measurements only when it was clear that the potential had stabilized (omitting the first days). To compute the

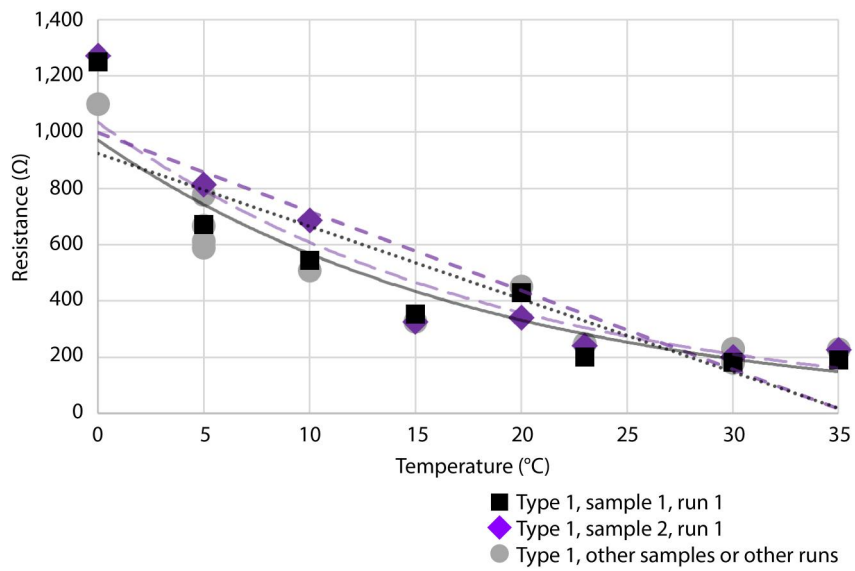

Figure 10. Variation of the electrical resistance with temperature for electrodes with the electrolyte and clay formula and ceramic plugs (type 1). Black squares are measurements for sample 1 (electrode #9); purple diamonds are for sample 2 (electrode #21). The gray circles are repeated measurements for other times and for other electrodes, to show the distribution of measurements. Linear best fit lines (black dotted line and purple dashed line) are shown, with best fit R-squared values greater than 0.87. Exponential best fit lines are also shown (purple long dashed line and black solid line). The linear slope from 5 to 30°C is −20 to −25 Ω/°C.

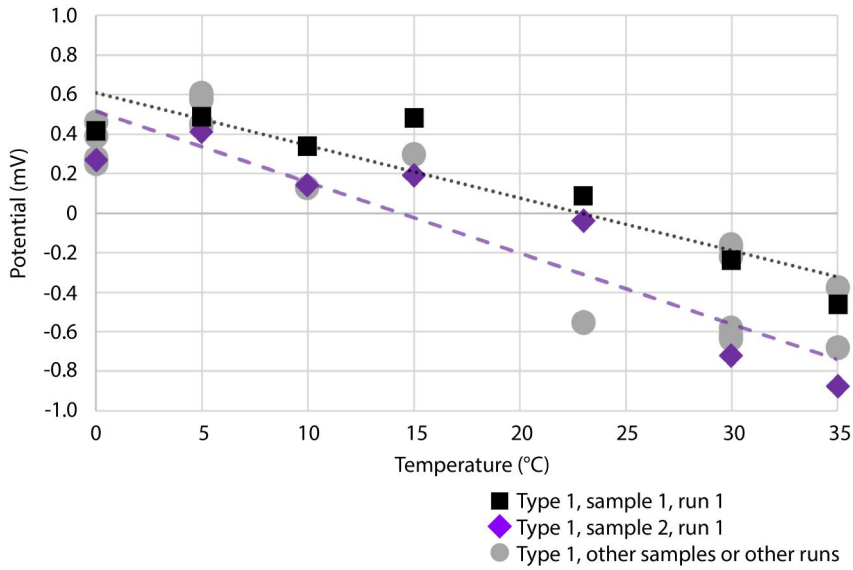

Figure 11. Variation of the electric potential with temperature for electrodes with the electrolyte and clay formula and ceramic plugs (type 1). Black squares are measurements for sample 1 (electrode #9); purple diamonds are for sample 2 (electrode #21). The gray circles are repeated measurements for other measurement runs done at different times and for other electrodes, to show the distribution of measurements. Linear best fit lines (black dotted line and purple dashed line) are shown, with best fit R-squared values greater than 0.84. The linear slope from 0 to 35°C is approximately −30 μV/°C.

variation of the electric potential with temperature, also known as the temperature effect or temperature coefficient, we take the difference of potentials measured at different temperatures and divide by the temperature change. A linear slope can be approximated over all the data, from 0 to 35°C. We compute a line with a slope of −25 (units μV per degree Celsius) for electrode #9 and a slope of −33 for electrode #21 (others tested followed a similar pattern). The fit of a linear trendline to the data has an R-squared value above 0.84. Repeated measurements at the same temperature show similar values for each individual electrode: the standard deviation ranged from 1% to 10% of the (mean) value, with a total average of about 5% (e.g., a standard deviation of 7 μV for measurements at 5°C, with a measurement separation of 1–4 hr).

A second experiment was carried out varying the temperature from 10 to 20°C and from 20 to 10°C. This gave a temperature coefficient of −34 and −28 μV/°C, respectively (averaged over several electrodes and several measurements). This value is quite small, showing that the temperature effect, and thus sensitivity to temperature variations, for this type of electrode is weak. The choice of a thick-walled canister and good seals with rubber O-rings may help to contribute to this. Petiau (2000) found a temperature coefficient of 30 μV/°C or less for their electrodes, and found that this was stable within a range of pH values. Our results here are consistent with their study. Petiau (2000) show that lead–lead(II) chloride electrodes with NaCl salt have a higher temperature coefficient than those with KCl salt, of about 230 μV/°C. Some commercially available lead–lead(II) chloride electrodes advertise a temperature coefficient of 40–210 μV/°C. Petiau and Dupis (1980) note that the temperature coefficient of lead–lead(II) chloride electrodes are significantly lower than other varieties, such as copper–copper(II) sulfate or silver–silver chloride electrodes (the latter are about −400 or −450 μV/°C). Petiau (2000) note that some of the preceding varieties can be 700–900 μV/°C. Petiau and Dupis (1980), who used Pb–$PbCl_2$ electrodes for magnetotelluric measurements with 100 m long dipoles, noted that the diurnal telluric variation in the field was about 200 μV (or 2 mV/km) and that the differences in temperature between the two electrodes set in the soil was on the order of 0.1°C giving a thermal drift on the order of 5 μV, which was many times smaller than the signal measured.

In a further test, the same procedure described above was carried out for the electrodes with the electrolyte only (type 2). The conditions and experimental procedure were the same. The measurements were made over a time span of 33 days (from 02 February 2023). The temperature was varied systematically from a minimum of 5°C to a maximum of 35°C. The variation of the resistance with temperature for this type of electrode was found to be

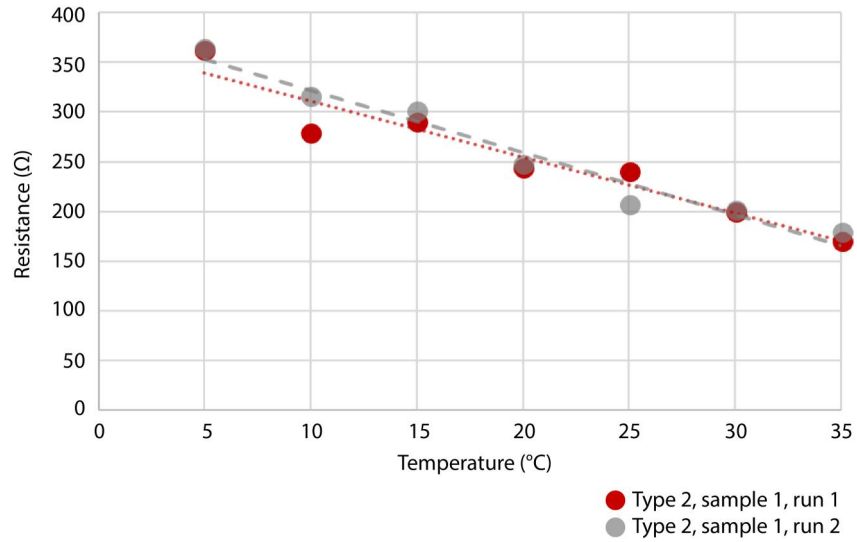

Figure 12. Variation of the electrical resistance with temperature for electrodes with electrolyte only (no clay) and ceramic plugs (type 2). Points are measurements for a pair of electrodes. The experiment was repeated in a second run at a different time to show the distribution of measurements. Linear best fit lines (red dotted line and gray dashed line) are shown, with best fit R-squared values greater than 0.92. The linear slope from 5 to 35°C is −6 Ω/°C.

−6 Ω/°C (Figure 12), from a linear slope approximated from 5 to 35°C. This is less than that found above for the electrodes with the electrolyte and clay formula (type 1). Additional measurements were carried out for the case of 0°C, where the medium contained some surface ice, and showed that the resistance increased to 525–600 Ω. The variation of the electrical potential with temperature for this type of electrode was found to be −30 μV/°C (Figure 13), from a linear slope approximated from 5 to 30°C. This is similar to that found for the electrodes with the electrolyte and clay formula (type 1).

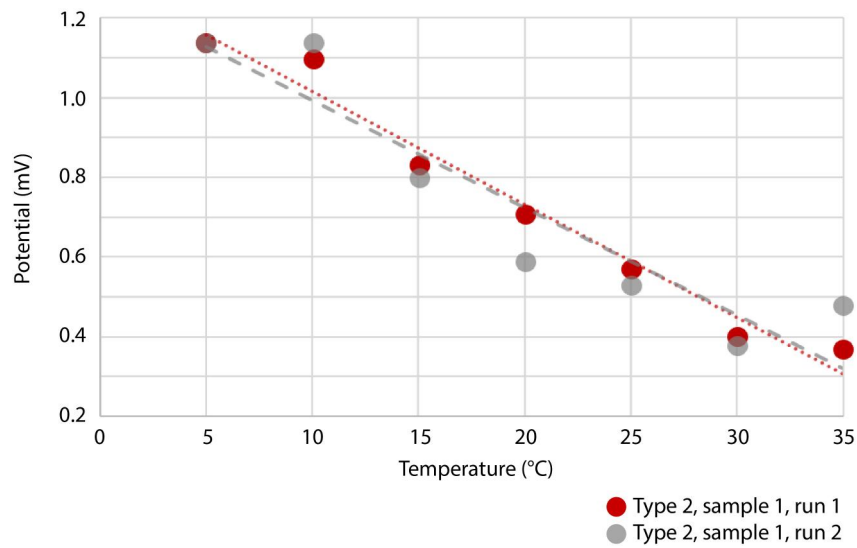

Figure 13. Variation of the electric potential with temperature for electrodes with electrolyte only (no clay) and ceramic plugs (type 2). Points are measurements for a pair of electrodes. The experiment was repeated in a second run at a different time to show the distribution of measurements. Linear best fit lines (red dotted line and gray dashed line) are shown, with best fit R-squared values greater than 0.87. The linear slope from 5 to 30°C is −30 μV/°C.

Table 4
Noise of Electrodes at Select Periods

Type	Standard deviation of electrical potential (μV)		
	Period: 1 s	Period: 120 s	Period: 3,600 s
Electrolyte and clay, ceramic plug (type 1; #012–21)	0.22	0.40	2.7
Electrolyte and clay, ceramic plug (type 1; #9–48)	0.21	0.32	1.9
Electrolyte and clay, wood plug (type 1b; #W1–W2)	0.33	0.30	4.5
Electrolyte only, ceramic plug (type 2; #L1–L2)	0.16	1.6	12

Note. Noise is defined as the standard deviation of the electrical potential for a zero mean.

4. Measurements of Noise and Stability

4.1. Noise: Variations in the Potential of an Electrode Over Short Time Scales

Continuous monitoring of the electrodes in a bucket of salt water (KCl with 5% saturation, about 17 g KCl in 1 L of water) was carried out. The measurements were made over a time span of ∼40 days (from 02 December 2022 to 10 January 2023) using a data logger (described by Becken et al., 2014) with a sampling rate of 128 Hz. Variations in the potential were analyzed over both short and medium time scales to gain a quantitative understanding of the noise. We define the noise as the standard deviation of the electrical potential measured at a select period when the mean is zero. Note that for a zero mean the standard deviation is similar to a root mean square error. We looked at measurements with a period of 1 s, 2 min (120 s), and 1 hr (3,600 s) and took a data set with up to 20 measurements at two or more separate times. Petiau and Dupis (1980) note that for good quality electrodes with low noise the noise of the amplifier usually dominates for frequencies above 5 Hz.

The noise of the electrodes described in this work was found to be very small for all electrode types at a period of 1 s, about 0.2–0.3 μV. The noise level is comparable to that described by Petiau and Dupis (1980): 0.4 μV for 1 s. The determined noise (averaged over multiple measurements and times) is summarized for each electrode type and each period in Table 4. Figure 14a shows the difference of the electric potential measurements and the mean for different types of electrodes at different times. For example, for the electrode with the electrolyte and clay formula with ceramic plug #9, all variations are within 0.2 μV of the mean. Note that the mean may be different for each time window.

For a period of 120 s, electrodes that used the electrolyte and clay formula (type 1) had a consistent noise level of 0.3–0.4 μV. In contrast electrodes with electrolyte only (type 2) were found to have a noise of 1.6 μV, on average. Although this was seen to vary; some time intervals showed a noise as low as 0.4 μV (Figure 14b), similar to that of the electrodes with the electrolyte and clay formula. The noise level is not unsimilar to that described by Petiau and Dupis (1980): 1.2 μV for 100 s. Overall, the noise level is much lower than some commercially available electrodes (1–10 μV).

For a period of 3,600 s, the noise increased significantly for all electrode types (Figure 14c). For electrodes with the electrolyte and clay formula (type 1), the noise was consistently 2–5 μV. For electrodes with the electrolyte only (type 2), the noise was about 12 μV, on average. Although this was seen to vary; some time intervals showed a noise as low as 2.5 μV. The lower noise level and the more consistent noise level of the electrodes with the electrolyte and clay formula compared to the electrodes with electrolyte only is an advantage. However, to put this in context, Petiau and Dupis (1980) note that a telluric line placed on the ground and oscillating in the wind (i.e., not buried or fixed, but loose) may create 10 μV of noise (by induction in the earth's magnetic field). One potential way to reduced such an effect is to use shielded cables.

4.2. Stability: Variations in the Potential of an Electrode Over Long Time Scales

Typically, for some time (order of hours) after the electrode is installed in a medium (e.g., soil) there is a period of variation, or drift, before stabilization related to the chemical equilibrium. However, variation or drift over long time scales can occur after this stabilization as well. Monitoring of the electrodes in the laboratory was carried out over ∼40 days (from 02 December 2022 to 10 January 2023; conditions as described above in Section 4.1) to assess the long-term stability of the potentials measured with the different electrode types. We took discrete

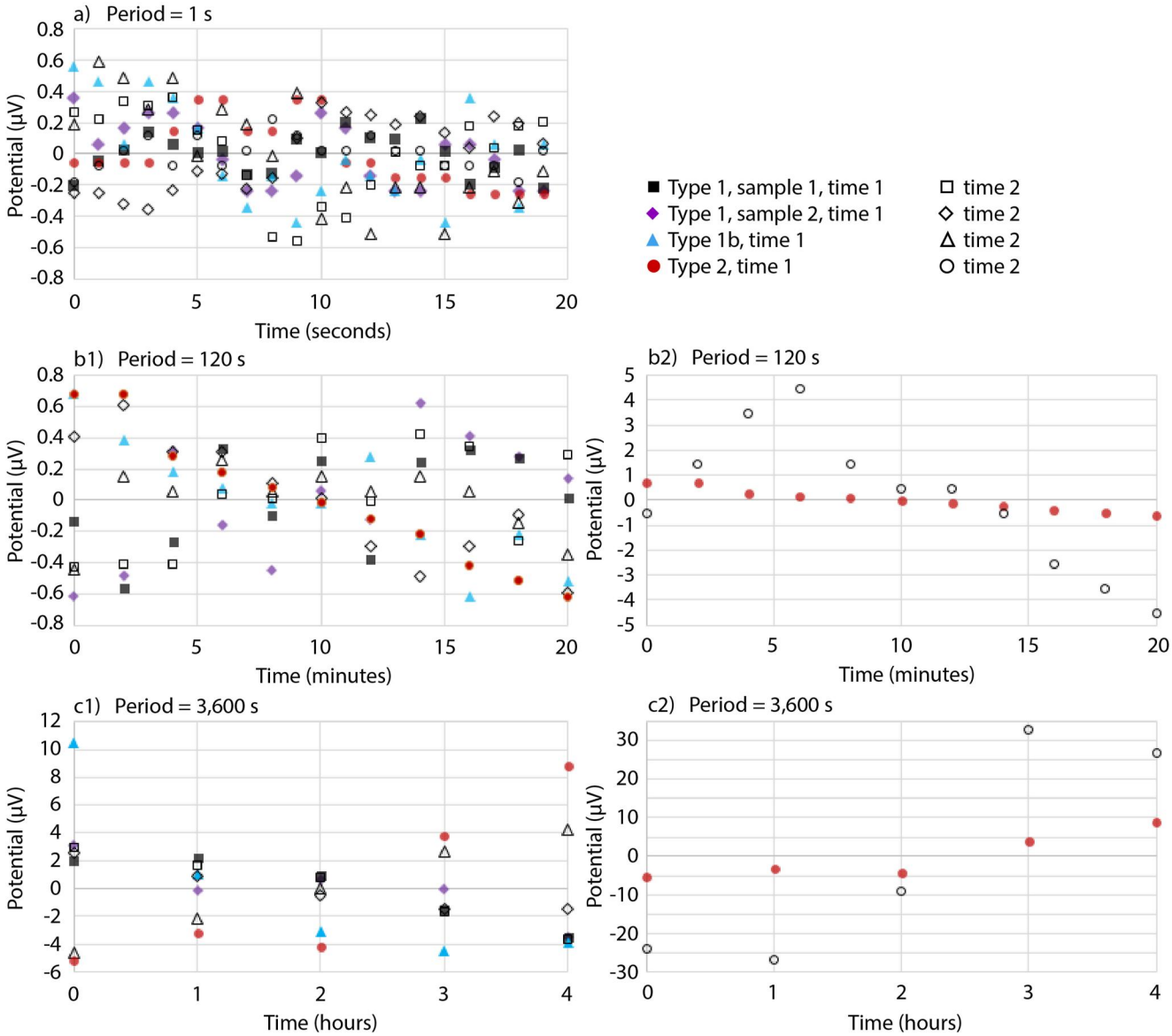

Figure 14. The difference of the electric potential measurements and the mean over selected periods for different types of electrodes. (a) Measurements taken 1s apart; (b) Measurements taken 120s apart (second panel for type 2 electrodes due to change of axis scale); (c) Measurements taken 3,600s apart (second panel due to change of axis scale). Symbol denotes electrode type; the symbol fill is for the measurement run carried out at a different time, color fill for time 1 and empty fill for time 2. Electrode pair with (i) electrolyte and clay formula and ceramic porous plugs (type 1; #012–21) shown with diamonds (purple), ii) electrolyte and clay formula and ceramic plugs (type 1; #9–48) shown with squares (black), iii) electrolyte and clay formula and wood plug (type 1b; #W1–W2) shown with triangles (blue), iv) electrolyte-only (no clay) and ceramic plugs (type 2; #L1–L2) shown with circles (red). Time 1 is measured from midnight 14 December 2022 and time 2 is measured from midnight 17 December 2022. At short periods (e.g., 1s) the variations are small for all electrode types; at longer periods (e.g., 3,600s) they become larger. Note the unit is μV, which is 0.001mV.

measurements with a nominal period of 1 day, however there were some gaps in the data over certain time frames (e.g., holidays and weekends; day 21 corresponds to 23 December 2022).

The electrodes with the electrolyte and clay formula (type 1 and type 1b) appeared to stabilize over the first week or so. In that time the drift could be approximated as linear and is −0.1, −0.6, and 0.2 mV for the three samples (day 2–9; black, purple, and blue on Figure 15a). In the following stable time they show a slight drift of −0.06, −0.46, and 0.06 mV/month (day 9–39; black, purple, and blue on Figure 15a). Over the whole time span, including the first week, the absolute drift ranged from 0.12 to 0.84 mV/month.

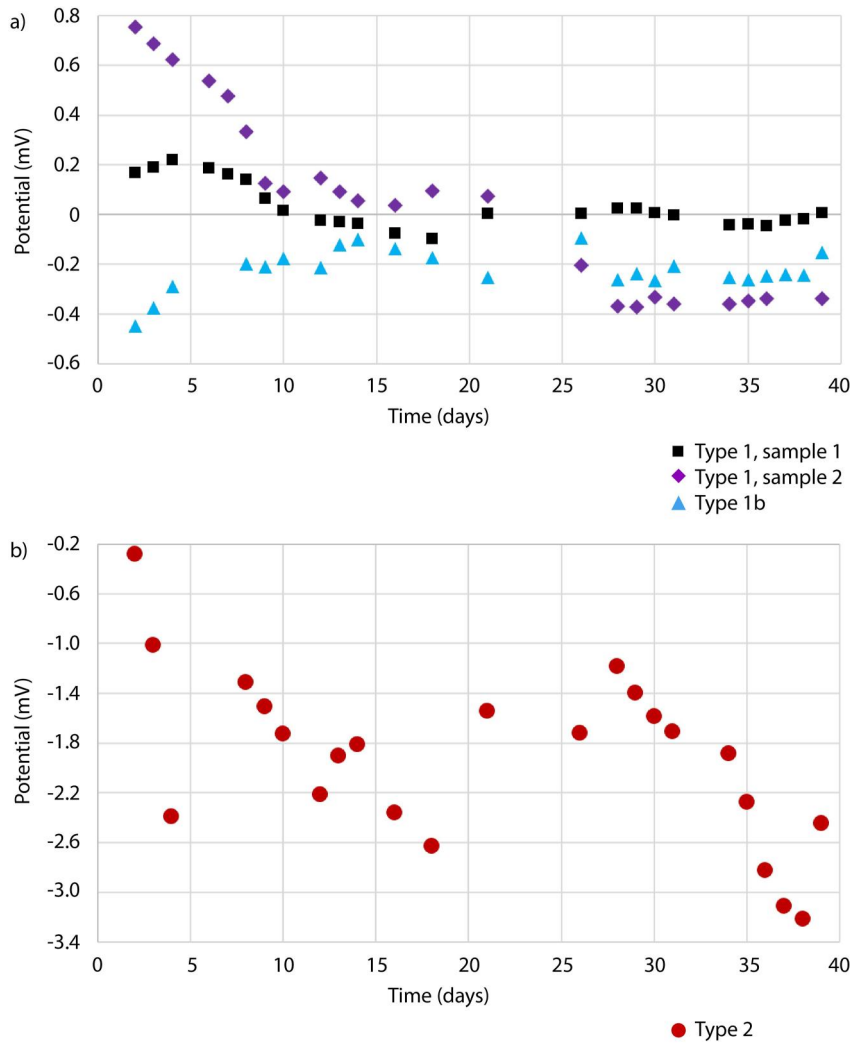

Figure 15. Long-term variations in the electric potential observed over more than 1 month for different types of electrodes. Discrete points were extracted from continuous measurements with a data logger. Panel a shows an electrode pair with i) the electrolyte and clay formula and ceramic plugs (type 1; sample 1 = #9–48) with black squares, ii) the electrolyte and clay formula and ceramic plugs (type 1; sample 2 = #012–21) with purple diamonds, and iii) the electrolyte and clay formula and wood plugs (type 1b; #W1–W2) with blue triangles. Panel b shows an electrode pair with the electrolyte only (no clay) and ceramic plugs (type 2; #L1–L2) with red circles. Note the y-axis scale is double that of panel a. Time is measured from 12:0:0 02 December 2022. Day 21 corresponds to 23 December 2022. Electrodes with the electrolyte and clay formula in panel a show a relatively smooth drift of 0.05–0.5 mV/month, after stabilization. In contrast, the electrodes with electrolyte only in panel b show much scatter and exhibit variations of 1–2 mV/month.

The drift level observed is comparable to that described by Petiau (2000), which is about 0.2 mV/month, and is not unsimilar to that described in Perrier et al. (1997) for several types of electrodes, which is about 0.1–1 mV/month. Petiau (2000) described how variations in the potential with time, or a drift, can be caused by variations of the internal electrode pH with time. For some electrodes, for example, #9 with the electrolyte and clay formula and a ceramic plug (black squares in Figure 15a), the drift was very subtle (after the first week) and could instead be considered as noise of about 37 μV (with a period of ∼1.5 days or ∼130,000 s; computed from the standard deviation with a zero mean).

In contrast, the electrodes with the electrolyte only (type 2) showed variations over the ∼40 days that were quite scattered and not smooth with a total variation of 1–2 mV/month (Figure 15b). For this type of electrode, Petiau and Dupis (1980) describe a drift of about 1 mV/month (with no change in the rate observed after 1.5 years of

monitoring). If it was considered instead to be noise it would be about 580 μV (with a period of ∼1.5 days or ∼130,000 s). Thus one advantage of the electrodes with the electrolyte and clay formula appears to be better long-term stability, with variations on this time scale having smaller, smoother, and more linear drifts (i.e., predictable).

4.3. Instabilities: Spikes and Steps in Laboratory and Field Measurements of the Electric Potential

The continuous time series recording made in the laboratory, using a data logger with a sampling rate of 128 Hz, shows the same observations discussed above for discrete measurements (Figure 16; unfortunately, not all of the data loggers were always operational and thus there are some gaps in the coverage). In the laboratory data (measured in an isolated bucket of salt water, see above) instabilities in the form of spikes in the potential, steps, and spontaneous jumps of unknown origin are observed.

Kanglin and Macnae (1998) observed that the stability of electrodes measured in a laboratory experiment was an excellent predictor of the stability of electrodes in the field. Field testing is complicated by the fact that the system is no longer in isolation. Long-term telluric measurements were carried out in the field in the Sauerland region of Germany (near the village of Oeventrop), and included redundant parallel dipoles to ensure consecutive stable time windows. Over a 15 day segment (from 01 December 2022) the weather was dry, except for moderate to heavy rain on day 7 and day 8. Instabilities in the form of spikes in the potential, steps, and spontaneous jumps of unknown origin were observed (Figure 17).

Variations in the potential over time can be caused by (a) physical changes in the contact between the electrode's porous membrane and the ground, and (b) changes in the chemical composition of the electrolyte within the electrode, such as a variation in the pH with time (Petiau, 2000) or leaking of the electrolyte and/or changes in the chemical concentration of the electrolyte (Kanglin & Macnae, 1998), as well as c) changes to the metal surface within the electrode, due to the accumulation of salt and/or degradation with age (e.g., see Figure 4). These variations can be slow and smooth and can appear as linear drifts. According to Kanglin and Macnae (1998), sudden or sharp variations (which they note can be more than 10 mV) are likely attributed to electrochemical

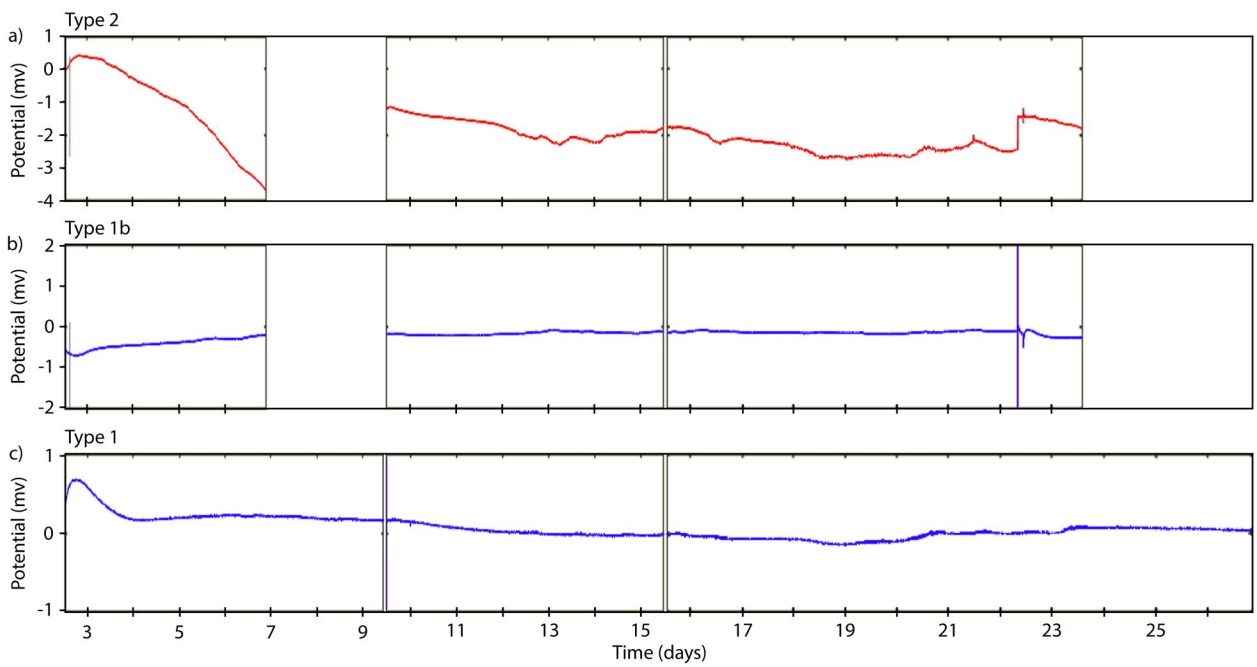

Figure 16. Continuous time series of the electric potential measured in the laboratory over several weeks for different types of electrodes. (a) The potential between two electrodes with electrolyte only and ceramic plugs (type 2; #L1–L2). Here a drift is observed, some oscillations, and a spontaneous jump (all on the order of 1mV). (b) The potential between two electrodes with the electrolyte and clay formula and wood plugs (type 1b; #W1–W2). (c) The potential between two electrodes with the electrolyte and clay formula and ceramic plugs (type 1; #9–48). Note that it stabilizes over the first day. Intra-day variations are small: less than 0.1mV. The sampling rate was 128Hz but 1Hz is shown here. Time is measured in days from midnight 30 November 2022 (equivalently, days of December).

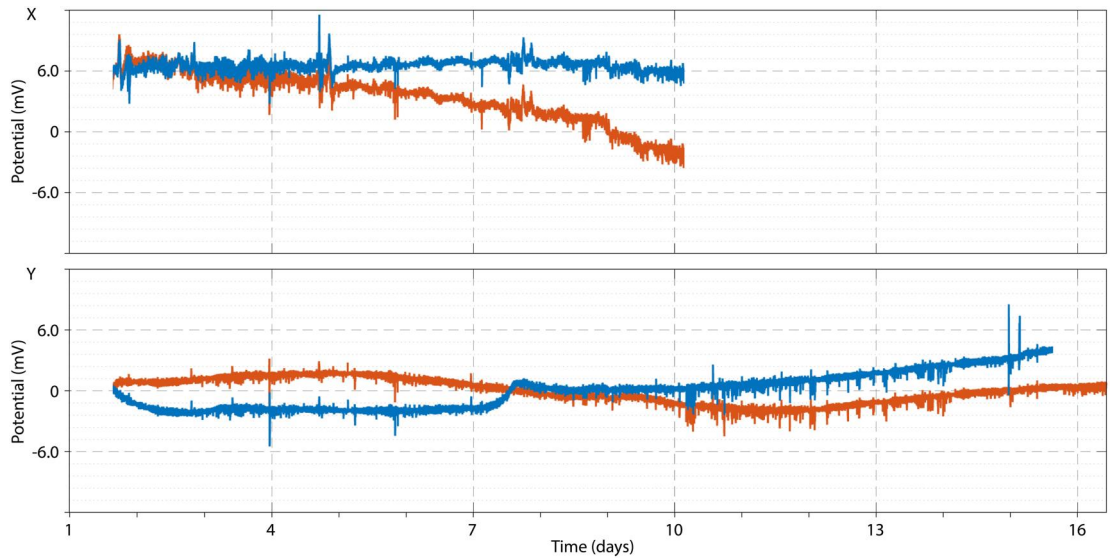

Figure 17. Time series of the electric potential measured in the field. Measurements were made on two parallel dipoles (blue and orange), in two orthogonal horizontal directions (X, north–south; Y, east–west), with 60m dipole lengths. Between parallel dipoles, a drift is observed and a step (on the order of several mV). Measurements were made with new porous-pot electrodes with the electrolyte and clay formula and ceramic porous plugs (type 1). The measurements come from long-term telluric recordings acquired in the Sauerland region of Germany (near the village of Oeventrop; approximately 51.4°N and 8.2°E). The sampling rate shown here is 64Hz. Time is measured in days from midnight 30 November 2022 (equivalently, days of December).

processes within the electrodes themselves, such as reaction charge release and charge accumulation. It should be noted that the electrochemical processes are not fully understood (Kanglin & Macnae, 1998).

Furthermore, drifts and offsets between different electrodes can be related to variations or changes in the inserted medium, including in moisture and salinity, due to, for example, water percolation effects after rainfall. Installing the electrodes in a homogenous material, such as a bentonite clay (which also improves the contact resistance between the electrode and the ground), can make the measurements less sensitive to local conditions and small-scale heterogeneities (Petiau, 2000) and is often used as an attempt to ensure constant moisture and salinity at the contact between the electrode and the ground. However, Hu et al. (2020) note that doing so may lead to certain unpredictable electrodiffusive effects as the homogenous material (e.g., bentonite) equilibrates with both the soil and the electrode, possibly causing an offset in the potential with respect to other electrodes or a strong drift.

4.3.1. Temperature Variation at the Electrode

The field measurements described above also monitored the temperature every hour with a small logging device (Figure 18) at two locations: (a) the bottom-hole temperature at a depth of 80 cm in the soil below the surface, where the electrode was planted, and (b) the top-hole temperature just below the surface at a depth of approximately 5 cm or less. The elevation of the measuring location is approximately 250 m above sea level. The recorded temperatures can be compared to the mean daily air temperature (from minimum and maximum) recorded nearby in the village of Oeventrop.

The first measurements (Figure 18a) show that daily temperature variations are observed at the shallow depth of ∼5 cm, often with minor peaks mid-day after noon. Some variations are on the order of 1°C over the time span of a day. These variations could affect telluric recordings if the electrodes were not planted at a sufficient depth. The values of the top-hole temperature range, in total, from about 0–6°C. At the greater depth of 80 cm, the temperature profile is smooth, and the seasonal trend of decreasing air temperature is followed. Daily minimum and maximum recorded air temperature is only 2°C from the mean value, on average. The values of the bottom-hole temperature range from about 6 to 8°C (i.e., warmer than the surface, due to a temperature delay). After day 18 (18 December 2022), the daily mean air temperature increased by a large amount, more than 17°C. The bottom-hole temperature decreased with a less steep slope, whereas the top-hole temperature increased by more than 3°C.

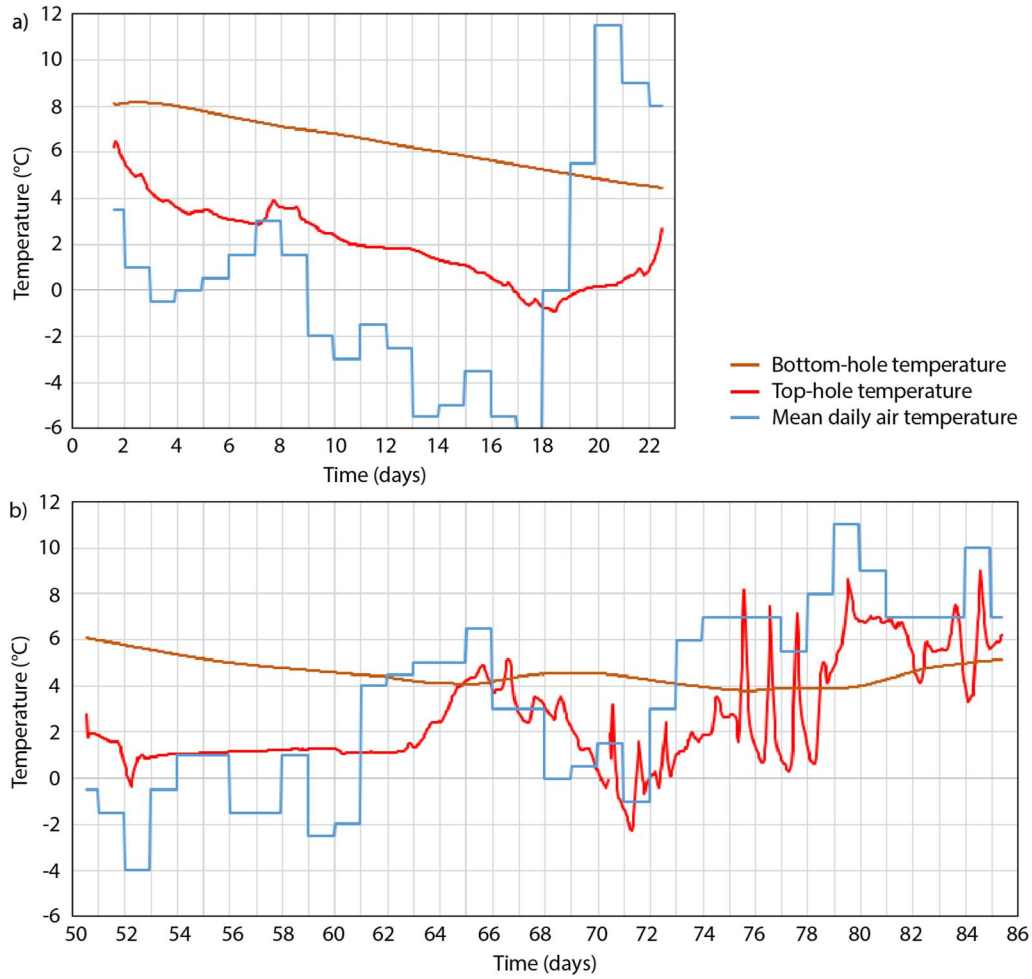

Figure 18. Temperature variation at the electrode, acquired during field measurements in the Sauerland region of Germany (near the village of Oeventrop; approximately 250 m above sea level). Orange line is the data from a temperature logger installed in the soil at the electrode depth of 80 cm below surface ("bottom-hole temperature"). Red line is the data from a temperature logger installed just below the surface at a depth of approximately 5 cm ("top-hole temperature"). Measurements are hourly. The blue line shows the mean daily air temperature (from minimum and maximum) recorded nearby in the village of Oeventrop. Measurements are from: (a) 1 December to 22 December 2022 and (b) 19 January to 8 February 2023 (day 70) and 8 February to 23 February 2023. There is a gap of temperature logger data in between the two campaigns, due to unforeseen technical issues. Time is measured in days from midnight 30 November 2022.

The second set of measurements (Figure 18b) shows similar results. Measurements started on day 50 (19 January 2023), due to a technical issue and therefore there is a gap in the data, and continued until day 70 (8 February 2023). The first part, during a cloudy January, shows little daily variations. The later part (after day 63; corresponding to 01 February 2023), shows the top-hole temperatures, which range in total from 0 to 5°C, increasing with the air temperature, and passing above the bottom-hole temperature. Furthermore, they show spikes that are on the order of 1°C over the time span of a day. The values of the bottom-hole temperature range from 4 to 6°C. Again, the daily minimum and maximum recorded air temperature is only 2°C from the mean value.

The third set of measurements (Figure 18b), day 70 to day 86 (8–23 February 2023), shows top-hole temperatures with significant daily variations, due to sunny weather, minimal clouds, and a seasonal warming trend. The daily minimum and maximum recorded air temperature on half the days had a range of 8–15°C. Top-hole temperatures, at ∼5 cm depth, show spikes of up to 7°C over the time span of a day. In total, top-hole temperatures range from −2 to 9°C, increasing over time with the trend of the air temperature, and passing above the bottom-hole

temperature. The values of the bottom-hole temperature, at 80 cm depth, range from 4 to 5°C. They show a delayed response from the air temperature trend of several days.

The results show that, (a) temperatures at a depth of 80 cm exhibit smooth trends (1–2°C/10 days) and no daily variations, in contrast to those at a depth of 5 cm, where daily variations can be quite appreciable (spikes of up to 7°C), (b) the temperatures at a depth of 80 cm were up to 6°C warmer than those at 5 cm depth, and (c) the temperatures at a depth of 80 cm did not go near 0°C over the winter months, despite some (about half) of the days having an air temperature less than or equal to 0°C, whereas at a depth of 5 cm the temperature did dip below 0°C at some times.

5. Summary and Conclusions

In this study, we describe the design and construction of a modular, refillable, non-polarizable porous-pot electrode. Such electrodes are used to measure a potential difference (voltage) between two points on the Earth (from which telluric currents are generated) and are used in many geophysical and geotechnical applications. We chose a chemical composition consisting of an over-saturated electrolyte solution stabilized in a clay, based on Petiau (2000). However, other electrolyte solutions are possible within the same design. We compare a formula with and without a clay base, different material for porous plugs, measure the sensitivity of the potential recordings to temperature, and assess the short-period noise and long-term stability of the electrodes. In addition, we show field data that highlights the application of the electrodes. We summarize the conclusions of the study below.

1. A modular design facilitates repair and allows to easily replace individual damaged pieces (such as cables or porous plugs) and to easily refill the electrolyte within the electrode as it degrades and dis-saturates over time.
2. Ceramic porous plugs are shown to have similar characteristics to wood plugs, including similar water flow-through rates, electrical resistances, and potentials. They are shown to produce similar results in long-term measurements in the laboratory.
3. Electrodes with the electrolyte and clay formula employed in this design have a low (weak) temperature sensitivity for the electric potential, about −30 μV/°C, measured by varying the temperature in a controlled environment from −3 to 35°C over 15 days. The temperature sensitivity was shown to be similar for electrodes with electrolyte only (no clay). The temperature sensitivity is much lower than some commercially available options (40–210 μV/°C) and comparable to that measured by Petiau (2000). Furthermore, according to Petiau (2000) and Petiau and Dupis (1980), it is significantly lower than the temperature sensitivity of Ag–AgCl or Cu–$CuSO_4$ electrodes, which can be 10 to 30 times higher.
4. The noise, defined as the standard deviation of the electric potential measured at a select period when the mean was zero, was found to be very small for all electrode types at a period of 1 s, about 0.2–0.3 μV, and for those with an electrolyte and clay formula (type 1) at a period of 120 s, 0.3–0.4 μV. Electrodes with the electrolyte only (type 2) were found to have a higher noise at a period of 120 s, 1.6 μV. For a period of 3,600 s, the noise increased significantly: 2–5 μV for electrodes with the electrolyte and clay formula (type 1) and about 12 μV for electrodes with the electrolyte only (type 2). The noise level is much lower than some commercially available options (1–10 μV) and comparable to that measured by Petiau (2000) (0.4–1.2 μV for 1–100 s). In general, the lower noise level, and more consistent noise level, of the electrodes with the electrolyte and clay formula compared to the electrodes with the electrolyte only is one reason why they are preferred.
5. Long term stability of the potentials measured was shown with laboratory measurements over 40 days. The electrodes with the electrolyte and clay formula (type 1) appeared to stabilize over the first week. In the following time they showed a smooth and slight drift of 0.05–0.5 mV/month. Over the whole time span the absolute drift ranged from 0.1 to 0.8 mV/month. In contrast, electrodes with the electrolyte only formula (type 2) showed a non-smooth pattern with a variation of 1–2 mV/month. This is one reason why it is preferred to use the electrolyte and clay formula over the electrolyte only.
6. During long-term field measurements, temperature logger data placed above the electrode at 5 cm depth and at the electrode at 80 cm depth showed that planting the electrode deeper avoids the daily variations of temperature, which can be appreciable (spikes of up to 7°C) and can affect the potential recordings. At the greater depth the temperature variation follows long-term seasonal trends (e.g., 1–2°C/10 days), but is insensitive to short-term variations. Furthermore, installing electrodes this deep can insulate them and avoid problems associated with the air temperature going below 0°C.

Data Availability Statement

The data used for analysis in this study are available in the Zenodo repository at https://doi.org/10.5281/zenodo.10474632 (Comeau, 2024).

Acknowledgments
Special thanks to Heinz Knese and the technical staff at the Institut für Geophysik, Universität Münster, for the initial designing, building, and testing of the electrodes through several iterations. We acknowledge the help of several students that collected field data in the Sauerland region of Germany. Questions on the study can be addressed to M.J. Comeau (M.J.Comeau@tudelft.nl). Open Access funding enabled and organized by Projekt DEAL.

References

Becken, M., Schmalzl, J., Bömer, B., & Ueding, S. (2014). Development of a E-field data logger and of time series processing tools in matlab. In *Abstracts for the 22nd Electromagnetic Induction Workshop (EMIW), Weimar, Germany*.

Comeau, M. J. (2024). Supplement to "Long-term stability, noise, and temperature sensitivity of modular porous-pot electrodes. [Dataset]. https://doi.org/10.5281/zenodo.10474632

Hu, K., Jougnot, D., Huang, Q., Looms, M. C., & Linde, N. (2020). Advancing quantitative understanding of self-potential signatures in the critical zone through long-term monitoring. *Journal of Hydrology*, *585*(2), 124771. https://doi.org/10.1016/j.jhydrol.2020.124771

Kanglin, L., & Macnae, J. (1998). The international campaign on intercomparison between electrodes for geoelectrical measurements. *Exploration Geophysics*, *29*(3–4), 484–488. https://doi.org/10.1071/EG998484

Perrier, F. E., Petiau, G., Clerc, G., Bogorodsky, V., Erkul, E., Jouniaux, L., et al. (1997). A one-year systematic study of electrodes for long period measurements of the electric field in geophysical environments. *Journal of Geomagnetism and Geoelectricity*, *49*(11–12), 1677–1696. https://doi.org/10.5636/jgg.49.1677

Petiau, G. (2000). Second generation of lead-lead chloride electrodes for geophysical applications. *Pure and Applied Geophysics*, *157*(3), 357–382. https://doi.org/10.1007/s000240050004

Petiau, G., & Dupis, A. (1980). Noise, temperature coefficient, and long-time stability of electrodes for telluric observations. *Geophysical Prospecting*, *28*(5), 792–804. https://doi.org/10.1111/j.1365-2478.1980.tb01261.x

Rigaud, R., Comeau, M. J., Becken, M., Kuvshinov, A., Tserendug, S., Batmagnai, E., & Demberel, S. (2023). Magnetotelluric data across Mongolia: Implications for Intracontinental Deformation and Intraplate Volcanism—Report on new measurements. In *Abstracts for the European Geophysical Union (EGU) General Assembly*. https://doi.org/10.5194/egusphere-egu23-9485

Rigaud, R., Comeau, M. J., Kuvshinov, A., Grayver, A., Batmagnai, E., Tserendug, S., et al. (2023). Extending magnetotelluric study from central to eastern Mongolia: Preliminary 2-D and 3-D inversion results. In *Abstracts for the International Union of Geodesy and Geophysics (IUGG) General Assembly Berlin 2023*. https://doi.org/10.57757/IUGG23-4312